2013

Rectifying differences in transport, dynamic, and quasi-equilibrium measurements of critical current density

I A. Golovchanskiy
University of Wollongong, ig684@uowmail.edu.au

A V. Pan
University of Wollongong, pan@uow.edu.au

O V. Shcherbakova
University of Wollongong, olga@uow.edu.au

S A. Fedoseev
University of Wollongong, sf477@uowmail.edu.au

Rectifying differences in transport, dynamic, and quasi-equilibrium measurements of critical current density

Abstract

The dependence of the critical current density (J_c) on electric field criteria (E_{cr}) is studied for high-quality YBCO ($YBa_2Cu_3O_7$) thin films over the entire applied magnetic field (B_a) range. The quantitative model describing the $J_c(B_a)$ dependence is compared and explained for the critical current densities obtained by different measurement techniques. Transport current and quasi-equilibrium magnetization measurement data can successfully be fitted by the model with appropriate electric field criteria. The dependence of the irreversibility field on the E_{cr} criterion can be obtained within the model. At the same time, the dynamic magnetization measurements of the $J_c(B_a)$ curves strongly depend on instrumentally defined parameters, introducing inconsistencies in the experimental results. Therefore, the model calculations are able to explain the $J_c(B_a)$ curves only if the instrumental vibrations affecting vortex behaviour are taken into account. However, the nature of the observed dependence on the vibration of the samples is unclear. Different frequencies of the sample vibrations have been investigated. It is revealed that if the frequency tends to zero, the $J_c(B_a)$ curves are well described by the model. We have outlined a number of possibilities which may be responsible for the behaviour observed. However, none of the existing theories can explain the effect of the vibrations, which exponentially degrade the irreversibility field to a certain tampered B_{irr} value at frequencies larger than $\simeq$25 Hz .

Keywords

density, current, measurements, rectifying, critical, differences, transport, dynamic, quasi, equilibrium

Disciplines

Engineering | Science and Technology Studies

Publication Details

Golovchanskiy, I. A., Pan, A. V., Shcherbakova, O. V. & Fedoseev, S. A. (2013). Rectifying differences in transport, dynamic, and quasi-equilibrium measurements of critical current density. Journal of Applied Physics, 114 (16), 163910-1-163910-9.

Rectifying differences in transport, dynamic, and quasi-equilibrium measurements of critical current density

I. A. Golovchanskiy, A. V. Pan,[a] O. V. Shcherbakova, and S. A. Fedoseev
Institute for Superconducting and Electronic Materials, University of Wollongong, Northfields Avenue, Wollongong, NSW 2522, Australia

(Received 9 August 2013; accepted 6 October 2013; published online 29 October 2013)

The dependence of the critical current density (J_c) on electric field criteria (E_{cr}) is studied for high-quality YBCO ($YBa_2Cu_3O_7$) thin films over the entire applied magnetic field (B_a) range. The quantitative model describing the $J_c(B_a)$ dependence is compared and explained for the critical current densities obtained by different measurement techniques. Transport current and quasi-equilibrium magnetization measurement data can successfully be fitted by the model with appropriate electric field criteria. The dependence of the irreversibility field on the E_{cr} criterion can be obtained within the model. At the same time, the dynamic magnetization measurements of the $J_c(B_a)$ curves strongly depend on instrumentally defined parameters, introducing inconsistencies in the experimental results. Therefore, the model calculations are able to explain the $J_c(B_a)$ curves only if the instrumental vibrations affecting vortex behaviour are taken into account. However, the nature of the observed dependence on the vibration of the samples is unclear. Different frequencies of the sample vibrations have been investigated. It is revealed that if the frequency tends to zero, the $J_c(B_a)$ curves are well described by the model. We have outlined a number of possibilities which may be responsible for the behaviour observed. However, none of the existing theories can explain the effect of the vibrations, which exponentially degrade the irreversibility field to a certain tampered B_{irr} value at frequencies larger than $\simeq 25$ Hz. © *2013 AIP Publishing LLC*. [http://dx.doi.org/10.1063/1.4826531]

I. INTRODUCTION

Superconductivity has advanced considerably over one hundred years since its discovery. A number of different superconducting materials has been discovered with different properties. These properties have to be established with various experimental techniques, which evolve and are persistently advanced to enhance sensitivity and uncover grey areas. As an example, critical current density (J_c) measurements (the most important practical characteristic) can be performed by direct transport current four-probe method, magnetization measurements,[1] analysing AC-susceptibility measurements,[2] and magneto-optical images.[3,4] Remarkably, in spite of the fact that during the J_c measurements by all these techniques a superconductor is in the critical state,[5] these measurements do not provide consistent results.

Fortunately, the thermally assisted processes obey a well known Arrhenius (Kim-Anderson) dependence.[5,6] This dependence is a self-sufficient approach that includes all types of vortex motion (thermally activated flux flow, flux creep, flux flow) without additional assumptions.[7–9] Moreover, it is possible to take into account pinning mechanisms within its general relation.[10] Any vortex motion in superconductors leads to the generation of the electric field. Differences in electric fields generated upon different measurements are responsible for different critical currents measured by different techniques, which is determined by the so-called electric field criterion (E_{cr}). Taking into account this criterion, the model describing critical current density behaviour for different measurement techniques has been proposed for $YBa_2Cu_3O_7$ (YBCO) thin films,[11] which is based on particular vortex pinning on extended defects, such as edge dislocations forming dislocation domain walls (grain boundaries) due to a small ($<3°$) misorientation angle between adjacent domains.[12–14] However, E_{cr} is not the only *instrumental* factor affecting measured critical currents. In addition to the small field and temperature inhomogeneities in the measurement systems, which were shown to strongly affect magnetization measurements,[15–18] tiny sample oscillations can dramatically affect J_c.[19] Thus, the main purpose of this work is unification of transport and magnetization critical current measurements, as well as explanation of the new phenomena arising due to low frequency sample oscillations in high quality YBCO thin films, which has never been reported in the literature.

Generally, changes in J_c dependence on the applied magnetic field (B_a) cause significant changes in the irreversibility field (B_{irr}). B_{irr} is a typical feature of high temperature superconductors,[10,20] which technically shows the irreversible limit of magnetization. It is hard to overestimate the importance of the irreversibility field in the science of superconductivity. On one hand, it can be an indicator for the melting transition from the flux line lattice to liquid,[21–23] or the crossover from the flux creep to the flux flow regimes,[24,25] or the depinning transition.[26] The irreversibility field can clearly be distinguished from the melting transition for Bi-based superconductors,[17] as well as for YBCO material near the critical temperature.[19] On the other hand, B_{irr} is

[a]pan@uow.edu.au

widely used for fitting $J_c(B_a)$ dependence,[27,28] as well as pinning force analysis through Kramer plots (originally proposed for conventional superconductors) employed for YBCO[29–31] and MgB_2[32,33] superconductors. In this paper, it will be shown that existing B_{irr} is an *instrumental* parameter, which strongly depends on measurement conditions, such as the electric field criterion and tiny sample oscillations at small frequencies. As a result, $B_{\rm irr}$ may not replicate a "fundamental" parameter, as well as it should be used with extreme caution for analysing parameters relevant for vortex pinning and critical current applications.

II. EXPERIMENTAL DETAILS

YBCO thin films were produced on 5×5 mm^2 $SrTiO_3$ (STO) substrates using standard pulsed-laser deposition (PLD) method[14,34] using KrF excimer laser with the wave-length of 248 nm. The PLD chamber was pre-evacuated down to 10^{-6} Torr. During the deposition, the substrate temperature and back oxygen pressure were 780 °C and 300 mTorr, respectively. The thin films measured in this work are of $d_p \simeq 450$ nm thick as determined by Dektak profiler. The critical temperature $T_c \simeq 89.5 \pm 0.5$ K was measured by DC magnetic measurements in Magnetic Properties Measurement System (MPMS) at $B_a = 2.5$ mT. The films were patterned into bridges 16 μm wide and 320 μm long by photolithography. The critical current density measurements were performed at $T = 77$ K by three different experimental techniques: (i) standard transport four-probe system employing Keithley nanovoltmeter and current source at two electric field criteria of 10^{-3} V/m (1 μV/cm) and 10^{-4} V/m (10 μV/cm); (ii) Quantum Design MPMS SQUID magnetometer by setting a magnetic field and measuring magnetic moment at the constant field in a quasi-equilibrium state; (iii) Quantum Design Physical Properties Measurement System (PPMS) Vibrating Sample Magnetometer (VSM) at different vibrating frequencies by sweeping the field at a constant sweep rate (dB_a/dt) and measuring the magnetic moment in the dynamic state. The critical current density (J_c) was determined from the magnetisation measurements using Bean formula for rectangular sample:[35] $J_c = 2\Delta M/[w_p(1 - w_p/3l_p)]$ in A/m^2, where w_p and l_p are, respectively, width and length of the samples measured, ΔM is the opening of hysteresis loops per unit volume. For YBCO films, $l_p = w_p = 5$ mm.

Magnetic measurements of J_c using PPMS have been also carried out for MgB_2 *bulk* superconductor, which was fabricated using *in situ* reaction technique as described in our previous works.[36–38] The dimensions of the samples are $1 \times 2 \times 3$ mm^3. The magnetic field is applied along the longest dimension $d_p = 3$ mm. To determine the critical current density, the same expression above[35] was employed with $l_p = 2$ mm and $w_p = 1$ mm. Different demagnetisation factors[39] for the film and bulk samples were not taken into account due to the following reasons: (i) the full penetration field is too small due to a huge demagnetising factor in the film geometry at perpendicular fields, hence the influence of the demagnetising factor is negligible over the entire field range; (ii) in the bulk sample, the influence of the demagnetisation factor is marginal at high fields, which is the region of interest for the MgB_2 sample in this work; and (iii) all the measurements were carried out with the same sample orientation with respect to the field.

III. $J_c(B_a)$ MODEL FOR YBCO FILMS

YBCO thin films grown by pulsed laser deposition possess different types of point, linear and planar defects.[40] Due to the Stranski-Krastanov growth mechanism,[41–43] epitaxial quasi-single-crystal thin films consist of domains. Misorientation angle between adjacent domains is expected to be much smaller than the critical angle of $\sim 3°$ at which the critical current density starts degrading due to the suppression of the superconducting order parameter.[44] The misorientation between the adjacent YBCO domains due to the growing and coalescenting YBCO islands and the misfit strains arising in the crystal lattice at the YBCO/STO interface[45] produces numerous out-of-plane edge and screw dislocations. These dislocations are most likely generated between growing islands of the films,[46] which may or may not be reflected at the film surface depending on it thickness and growth parameters. These dislocation would form low-angle domain boundaries between single-crystal domains of the epitaxially grown films,[43] which are likely to form rectangular-like patterns.[46] It has been shown[12,13,47,48] that out-of-plane edge dislocations are the most effective pins for Abrikosov vortex line lattice.

In this model, the domains are approximated by rectangles with an average domain size of $\langle L \rangle$. The domain walls of 2δ wide are considered to be the pinning area. Vortices located within this area along the domain walls are said to be pinned (Fig. 1). The ratio of the pinned vortices (n_p) to the total number of vortices (n_v), the so-called accommodation function, is given by[12,49]

$$\frac{n_p}{n_v} = 1 - \left(\frac{\Gamma\left(\nu, \frac{2\delta}{\mu}\right) - \frac{2\delta}{\mu}\Gamma\left(\nu - 1, \frac{2\delta}{\mu}\right)}{\Gamma(\nu)} \right)^2. \quad (1)$$

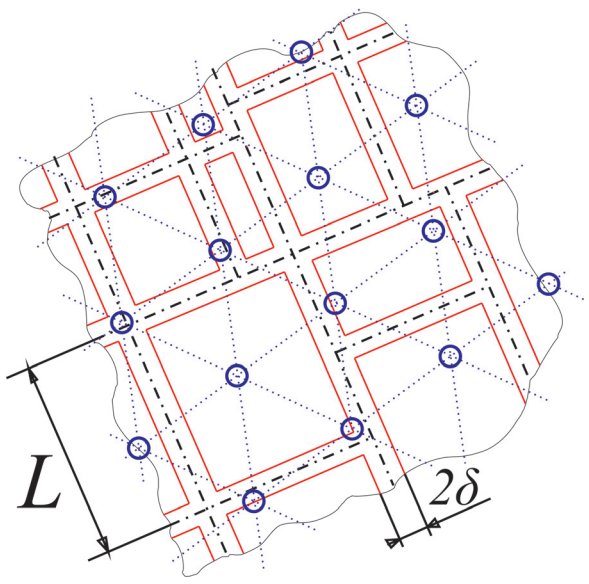

FIG. 1. Domains are approximated by rectangles with average size $\langle L \rangle$. Vortices (circles) within δ from domain walls (dash-dotted line) are pinned.

The accommodation function depends on the average domain size $\langle L\rangle$ via $\mu = \langle L\rangle/\nu$ with μ and ν being characteristic of domain size distribution. Parameter $\delta(B_a)$ is defined through the competition between vortex displacement energy in the flux line lattice (FLL) from its equilibrium position and pinning energy,[12]

$$\delta = \frac{r_0}{\xi(T)}\sqrt{\frac{\Phi_0}{B_a}}, \tag{2}$$

where r_0 is the dislocation core radius (assumed to be ~1 nm for calculations[12,47]), $\xi(T) = \xi_0/\sqrt{1-(T/T_c)^4}$ (Ref. 50) is the coherence length with $\xi_0 \simeq 2$ nm for the YBCO films,[47] and Φ_0 is the flux quantum.

Parameter δ clearly depends on the applied field and temperature. The temperature dependence in low fields was experimentally explored in Refs. 51 and 52. The field dependence requires considering a certain geometrical correction due to the varying shape of the pinning potential as follows.[49,53] If $2\delta < d$ (d is the distance between dislocations in a domain wall) each dislocation core in this boundary act as a single pinning centre. In this case, the probability for a vortex in the boundary zone to be pinned is the ratio of the pinning area around each dislocation $\pi\delta^2$ to the assumed rectangular pinning area of the boundary $2\delta d$. If $2\delta > d$, the entire domain wall acts as the pinning area because the pinning zones δ around dislocations overlap. Thus, the geometrical correction for these cases is given as[49,53]

$$K_{\mathrm{sh}} = \begin{cases} \dfrac{\pi\delta}{2d} & ,\dfrac{2\delta}{d} < 1 \\ \dfrac{\int_0^{d/2}\left(1-\left(\dfrac{x}{\delta}\right)^m\right)^{\frac{1}{n}}dx}{d/2} & ,\dfrac{2\delta}{d} > 1. \end{cases} \tag{3}$$

The product $K_{\mathrm{sh}}n_p/n_v$ provides the probability of vortex to be pinned. Along with the applied field and temperature, it strongly depends on structural parameters of thin film, such as the average domain size and distance between dislocations in the domain walls.[12] This product can be interpreted as the pinning potential U for one vortex,

$$U = U_0\frac{n_p}{n_v}K_{\mathrm{sh}}, \tag{4}$$

where $U_0 = \beta k_B T$ with k_B being Boltzmann constant and β—a free parameter. However, it should be noted that practically the overlap of the pinning potentials leads to weaker pinning between dislocations,[53] somewhat resembling the potential considered for twins as additional pinning centres in YBCO film[54] or even for the extreme regime of weak-links applicable to coated conductors.[53]

At high fields and/or temperatures, thermally activated processes play important role. As a result, significant flux creep occurs. We use Kim-Anderson approach to take this creep into account.[6,7,9] The velocity of the vortex creep is

$$V = a_0\nu_0\exp\left(-\frac{U}{k_BT}\right)\sinh\left(\frac{U_L}{kT}\right), \tag{5}$$

where $a_0 \sim \sqrt{\Phi_0/B_a}$ is the intervortex distance; while the driving (Lorentz) force potential U_L is assumed to be $\propto J_c/\alpha$ with α being a free parameter. ν_0 is the vortex vibration frequency, which was found to range from $10^5\,\mathrm{s}^{-1}$ to $10^{13}\,\mathrm{s}^{-1}$ according to the different sources.[6,7] ν_0 is limited by the atomic vibration frequency, hence it depends on temperature.

From Eq. (4), taking into account that vortex movement causes dissipation and electric field $\vec{E} = [\vec{V}\times\vec{B_a}]$ for the critical current density J_c, we obtain

$$J_c(B_a,T) = \alpha k_BT \times \mathrm{arcsinh}\left[\frac{E_{cr}}{a_0(B_a)\nu_0(T)B_a} \times\exp\left(\beta\frac{n_p}{n_v}(B_a,T)K_{\mathrm{sh}}(B_a,T)\right)\right]. \tag{6}$$

IV. ELECTRIC FIELD CRITERIA AND IRREVERSIBILITY FIELD FOR DIFFERENT MEASUREMENT TECHNIQUES

As can be seen from Eq. (6), the critical current is determined not only by pinning properties of the superconductor, but also by the electric field generated during measurement (E_{cr}, the so-called electric field criterion), which may strongly depend on the measurement technique employed. In this work, three different techniques with different criteria have been used to determine and compare $J_c(B_a)$ behaviour.

(i) One technique employed is the conventional DC four-probe method. For these measurements, our YBCO films have been patterned into bridges by photolithography. Electric field response was measured directly by nanovoltmeter during ramping up the applied current. The critical current was determined with two electric field criteria of 10^{-4} V/m and 10^{-3} V/m.

(ii) Another technique for the critical current determination was magnetization measurements[1] by Quantum Design MPMS SQUID magnetometer. Before taking magnetization measurement at each field set point, the magnetic field is swept with the rate of 2×10^{-2} T/s to the set point and stabilized in no-overshoot approach. To measure magnetization, the sample was scanned through the set of the SQUID pick up coils with the 4 cm scan length, the magnetization was averaged over 3 scans. Each scan takes approximately 40 s, while each measurement (from point to point) takes ~3 min. The unchanged magnetic field for high temperature superconductors (HTS) assumes significant relaxation processes,[55] which control vortex dynamics and electric field generation in HTS samples. The value of electric field in this case can vary from 10^{-7} to 10^{-12} V/m as was estimated theoretically in Refs. 56 and 57 and calculated from experimental data in Refs. 28, 58, and 59. In our MPMS experiments, the electric field criterion of 10^{-11} V/m was obtained by fitting the model to the J_c curve measured by MPMS. Whereas the naive estimation of this criterion by taking into account, the averaged MPMS field sweep rate gives $E_{\mathrm{cr}} \sim 10^{-6}-10^{-7}$ V/m. It is 4–5 orders of magnitude larger than

the one obtained through the model fit or found in the literature. The difference can likely be due to the non-linearity of the relaxation process in time. It leads to rapid relaxation after the field sweep has stopped for measurements, as also discussed in Refs. 55 and 59. On the other hand, the magnetic field sweep rate for changing B_a from one set point to another decreases significantly upon approaching the set point, additionally reducing E_{cr}.

(iii) A third technique employed in this work was magnetization measurements by Quantum Design PPMS VSM, which is significantly different from MPMS measurements in at least two ways as follows. (a) During measurements applied, magnetic field was continuously swept at constant rate from 10^{-3} T/s to 1.2×10^{-2} T/s, hence the sample measured is a dynamic state upon measurements in contrast to MPMS where the measurements occur in a constant field in a stationary (or quasi-static) state. (b) To measure the magnetization of the sample in PPMS VSM, the sample vibrates in the set of pick up coils at a certain frequency (f) and amplitude (the VSM default vibration settings are $f = 40$ Hz with 2 mm amplitude and 1 s averaging time per measurement), whereas in MPMS it is steadily scanned over a certain scan length (usually 4 cm). Thus, one measured value in PPMS is an average over period of time that depend on frequency and amplitude of vibrations. These parameters determine sensitivity of VSM.

As vortex dynamics upon PPMS VSM measurements depends on the sweep rate of magnetic field, the electric field generated as a result of this dynamics is also strongly dependent on the sweep rate (dB_a/dt). This electric field can be estimated as $E_{cr} \sim s/2 \times dB_a/dt$,[57] where s is the effective transverse size of the sample (relative to the field direction). In the case of our films having $s = 5$ mm, E_{cr} was estimated to be 3×10^{-5} V/m and 2.5×10^{-6} V/m for $dB_a/dt = 1.2 \times 10^{-2}$ T/s and 10^{-3} T/s, respectively.

It is interesting to compare irreversibility fields expected for the different measurement techniques considered in this work. Using Eq. (6), B_{irr} is plotted as a function of the electric field criterion in the logarithmic scale. To employ Eq. (6), parameters obtained in our previous work[11,60] were used. Fig. 2 shows that B_{irr} can change from ~2 T for the MPMS measurements to ~8 T for the transport current measurements as is usually observed in experiments found in the literature and as also observed in our work. Clearly, from Fig. 2 it can be concluded that B_{irr} (as well as the corresponding $J_c(B_a)$ curves) can significantly be altered for the transport measurements carried out at different criteria (the right shaded box in Fig. 2). MPMS measurements possess a much narrower range for the variation of the B_{irr} (the left shaded box in Fig. 2) due to performing measurements in a rather equilibrium vortex state. However, it is worthwhile noting that it is the most sensitive technique available. The E_{cr} range for the VSM PPMS measurements (the shaded box in the middle of the graph in Fig. 2) has been established for the sweep rates used in this work and for the film with 5 mm transverse dimension.

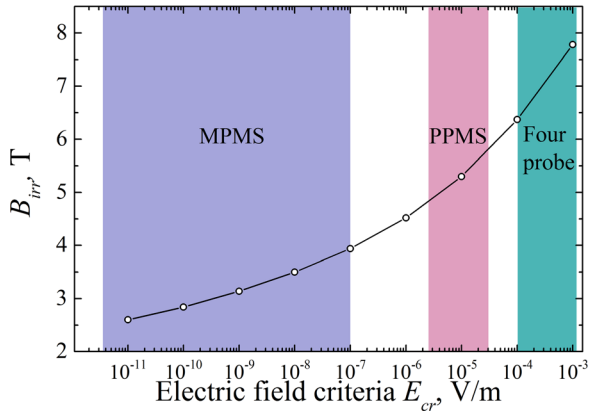

FIG. 2. The irreversibility field dependence on the electric field criteria at $T = 77$ K derived from Eq. (6). The irreversibility field was determined at the critical current density value of 3×10^7 A/m^2.

V. MEASUREMENTS DESCRIBED BY THE MODEL

We have measured the critical current density in a PLD YBCO thin film by three different techniques described above with 5 different E_{cr} in total: 10^{-11} V/m for MPMS; 10^{-4} V/m and 10^{-3} V/m for transport current; and 2.5×10^{-6} V/m and 3×10^{-5} V/m for PPMS VSM measurements. The results of the measurements are shown in Fig. 3. The model curves obtained by fitting the experimental curve with Eq. (6) are plotted using the corresponding criteria. As can be seen, the model reasonably well fits the results of transport current and MPMS measurements over the entire field range. At the same time, the model was unable to fit the PPMS results using the PPMS criteria employed. Although the general trend is reproduced, the experimental and model curves progressively diverge in increasing B_a. The irreversibility field exhibits a similar tendency. The B_{irr} values obtained from the model and experiment are rather consistent (within 15% difference) for MPMS and transport measurements, whereas for PPMS measurements the experimental B_{irr} values are about a factor of two smaller than

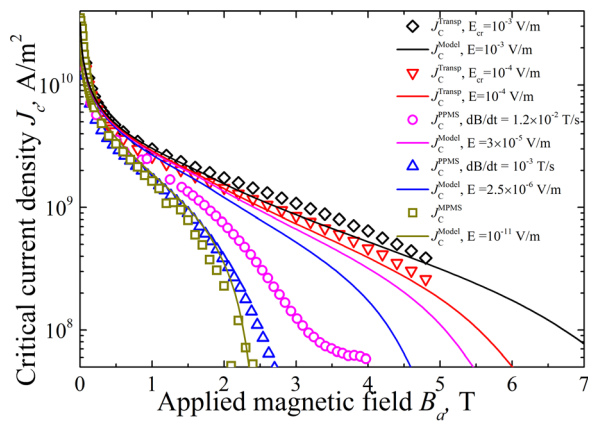

FIG. 3. The critical current density dependences (symbols) measured at $T = 77$ K as the function of the applied magnetic field with the corresponding fitting curves (lines) obtained from the model (Eq. (6)) using the appropriate electric field criteria.

those obtained within the model (Figs. 2 and 3). As we show below, this inconsistency between the PPMS measurements and the model arises from instrumentally driven factors, inducing new and unexpected vortex dynamics.

This problem appears to be quite common in the literature and in particular obvious if all three techniques were employed in one work.[28,58] For example, in Ref. 28, $E - J$ characteristics of YBCO films have been investigated using MPMS, PPMS VSM, and transport current measurements. The $J_c(E)$ results of PPMS VSM measurements are shifted towards lower J_c values from the united trend established by two other techniques as can be seen in Figs. 10, 11, and 15 of Ref. 28. These inconsistencies have never been explained.

VI. VIBRATION INFLUENCE ON J_c

As mentioned above, the sample vibrates within the pick-up coil with a certain frequency upon PPMS VSM measurements, whereas it is stationary in transport measurements and moves steadily during MPMS scans. The default frequency ($f = 40$ Hz) provides optimal conditions for high sensitivity of magnetometery and fast measurements. This frequency is not recommended to be altered by the manufacturer (Quantum Design)[67] due to a reduced sensitivity at lower frequencies and due to possibility to overheat the motor and cause problems with the VSM hardware at higher frequencies. However, as shown below, the influence of the frequency on the J_c and B_{irr} measurements is so dramatic that it needs to be taken into account for accuracy of the measurements and corresponding interpretations.

In Fig. 4, the parameters of the VSM measurements of magnetization as a function of magnetic field were kept the same except the frequency varied from 2 Hz to 60 Hz: 5×10^{-3} T/s, which corresponds to $E_{cr} \simeq 1.3 \times 10^{-5}$ V/m; vibration amplitude was 2 mm; time per measurement was 3 s (it was increased from the default of 1 s to provide higher sensitivity at low frequencies). The results reveal dramatic influence of sample vibration frequency on the critical current density calculated from the magnetization hysteresis loops. J_c decreases drastically with increasing f, and the deviations are more pronounced with increasing magnetic field.

It is natural to assume that the vibrations cause perturbations in vortex dynamics, induce relaxation processes leading to J_c degradation. If $f \to 0$, these perturbations become negligible and J_c measured tends to its transport current value corresponding to its E_{cr} criterion. These arguments are consistent with the model calculation obtained from Eq. (6) and shown in Fig. 4 as the line, which fits well the data obtained for the lowest frequency used ($f = 2$ Hz) in a sharp contrast to the VSM default settings as shown in Fig. 3. It also proves the integrity of the model as being independent of the instrumental and measuring artefacts.

It is important to note that for $f > 4$ Hz the $J_c(B_a)$ curves exhibit a tail at $B_a > 3$ T, which becomes more pronounced with increasing f (Fig. 4). This tale can exhibit a different regime for vortex pinning, vortex lattice phase, sample granularity and corresponding screening of the grains (as was done for MgB_2 bulk superconductor[61]), or perhaps even measurement artefact. Indeed, this kind of behaviour is not usually observed in transport current and MPMS measurements, so it may be an indication of the VSM measurement artefact or specific feature of the dynamic vortex state due to PPMS continuous field sweep.

To ensure that the frequency effect is not ruled by the aspect ratio of thin films or the specific type of the pinning in HTS YBCO films, we have also measured bulk MgB_2 and Nb samples. The results obtained are rather similar, so we demonstrate only results obtained for MgB_2 sample (Fig. 5) performed under the same instrumental conditions as for the YBCO film. The behaviour of the $J_c(B_a)$ curves measured at different frequencies is somewhat different than those measured for the YBCO film (Fig. 4). They do show the reduced B_{irr} values and lower J_c curves with increasing f as for the YBCO film, but they do not show the tail behaviour with the obvious crossover in the form of a kink. Another difference can be noticed in how the curves bunch up: for the MgB_2 sample, the curves tend to coincide below 3.5 T and above 3.5 T the curves progressively degrade faster with increasing frequency (in particular for $f > 25$ Hz); whereas for the YBCO film, the J_c curves degrade rapidly for at low frequencies $f < 25$ Hz and then bunch up at higher frequencies. It is

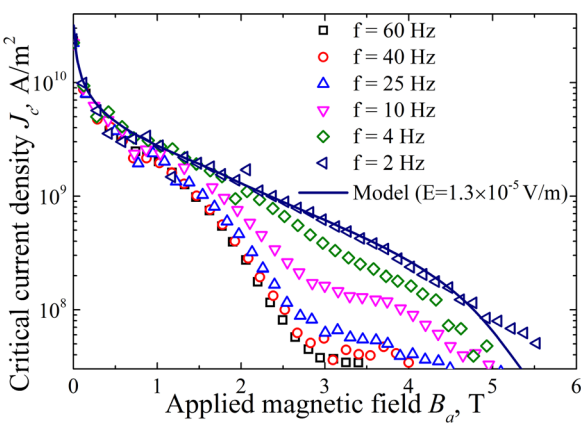

FIG. 4. Critical current density dependence on field of YBCO thin film at $T = 77$ K measured by VSM PPMS at field sweep rate 5×10^{-3} T/s and different frequencies f.

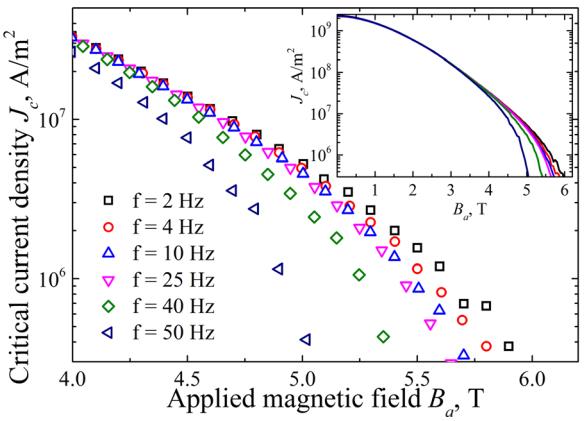

FIG. 5. Critical current density dependence on magnetic field in high field region for bulk MgB_2 at $T = 20$ K measured in PPMS at field sweep rate 5×10^{-3} T/s and different frequencies f. The inset shows the entire critical current density dependence on magnetic field.

important to emphasise that these results are obtained for the bulk sample with the absolutely different origin of the vortex pinning. This implies that vortex behaviour is responsible for the frequency dependence observed.

To gain the insight into this frequency driven behaviour, we have analysed the $J_c(B_a)$ curves obtained at different frequencies for YBCO film in Fig. 4. In general, it appears that the irreversibility field decreases with the frequency increase. However, the J_c behaviour is quite complex in particular for $f > 4$ Hz. The curves exhibit a kink at $B_a \simeq 3$ T, which may indicate a vortex pinning related transition. Using our model (Eq. (6)) to fit the low-field parts (up to 3 T) of these curves, we obtain the set of J_c curves as if there was no transition at 3 T. The $B_{\rm irr}$ has been obtained at the intersection of these curves with $J_c = 5 \times 10^7$ A/m^2. In Fig. 6, the so-obtained $B_{\rm irr}$ is plotted as function of PPMS VSM measurement frequency for three different field sweep rates. The data can be fitted with the following exponential expression:

$$B_{\rm irr}(f) = B^T_{\rm irr} + B^f_{\rm irr}(0)\exp(-f/f_d)\,, \tag{7}$$

where $B^T_{\rm irr}$ is the tempered value of the irreversibility field measured at high frequencies, f_d is a characteristic frequency of the irreversibility field decay, $[B^T_{\rm irr} + B^f_{\rm irr}(0)]$ is the irreversibility field of "undisturbed" superconducting sample, measured at $f \to 0$ Hz. Fitting parameters are shown in Table I.

Note, for the slowest sweep rate applied and at $f > 25$ Hz J_c determined by PPMS is very similar to the $J_c(B_a)$ obtained by the quasi-equilibrium MPMS measurements (Fig. 3). On the other hand, the J_c results obtained for the lowest possible frequency $f = 2$ Hz at small sweep rates are achieving values obtained by transport measurement, but they cannot be attained by the fastest available sweep rate in PPMS at frequencies $f > 25$ Hz (Figs. 3, 4 and 6 for irreversibility field comparison). This clearly separates the influence of these two measuring parameters, while it confirms the strong dependence on flux relaxation, flux dynamics, and corresponding $E_{\rm cr}$.

In order to explain this behaviour, the origin of this effect has to be understood, that is: Why the sample vibrating along the direction of the applied field experiencing changes in the vortex induced properties of the superconductors?

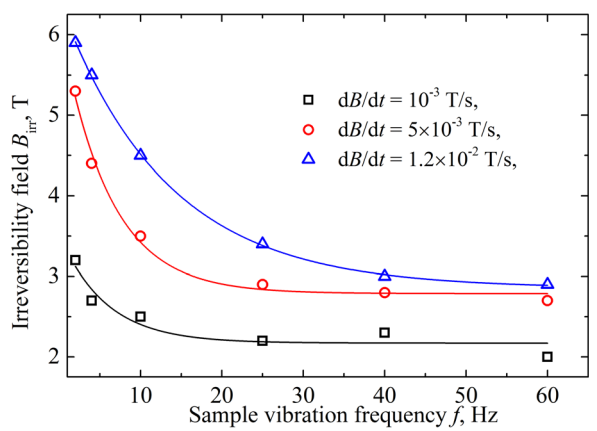

FIG. 6. Irreversibility field dependence on frequency at $T = 77$ K for three different sweep rates.

TABLE I. Parameters for Eq. (7) used to fit the experimental data.

dB_a/dt, $\times 10^{-2}$ T/s	$B^T_{\rm irr}$, T	$B^f_{\rm irr}(0)$, T	f_d, Hz
0.1	2.17	1.36	5.6
0.5	2.79	3.14	6.0
1.2	2.85	3.56	13.1

VII. THE ORIGIN OF VIBRATION-INDUCED PHENOMENA

To affect the flux line lattice, the vibrations of superconductors in homogeneous magnetic field of the PPMS VSM magnetometer have to induce additional propagation of vortex lattice driven by Lorentz force. Thus, the most straightforward source of this propagation would be inhomogeneities in the experimental environment or conditions, which are nominally assumed to be constant. Indeed, a number of works revealed the effects of small non-uniformities on magnetization. For example, in Ref. 62, it was shown that YBCO single crystal movements in a transverse magnetic field with inhomogeneities of ~0.005% led to some artefacts in magnetization curves and resulted in general decrease of the magnetization upon measurements in a MPMS. In Ref. 63, the level of such inhomogeneities in MPMS was investigated. It was shown that such inhomogeneities caused positive signal below T_c upon field cooled magnetization measurements as a function of temperature, the so-called paramagnetic Meissner effect (PME). In Ref. 15, the PME in YBCO thin films was studied in the framework of Koshelev-Larkin theory.[64] The key-idea of PME appearance suggested was inhomogeneous flux compression that can happen because of inhomogeneous superconducting transition. The source of such inhomogeneous transition is not important, but can be trigged by non-uniformities of the applied magnetic field and temperature.[15,65] All these works show that inhomogeneities play a crucial role in superconductor behaviour, and they are assumed as the main cause leading to the drop of $J_c(B_a)$ with frequency in our work.

In general, all inhomogeneities in measurement environment can be seen described as thermal and/or magnetic fluctuations. There are two possibilities for thermal perturbations: (i) the actual inhomogeneity of temperature in sample's space; and (ii) Bardeen-Stephen heating caused by periodic vortex motion[66] (if we assume that this motion is induced as a vibrations). Any additionally induced heating would lead to the drop of the potential pinning barrier, which is proportional to the density of moving vortices (i.e., B_a) and vibration frequency. Temperature dependence of $B_{\rm irr}$ was shown to be[24,25]

$$B_{\rm irr}(T) = B_{\rm irr}(0)(1 - T/T_c)^n\,, \tag{8}$$

where $n \simeq 3/2$,[10,62] $B_{\rm irr}(0)$ is the irreversibility field at zero temperature. Taking into account the $B_{\rm irr}(E_{\rm cr})$ curve in Fig. 2, the maximum temperature rise achieved by the sample vibrations can be roughly estimated with Eq. (8) to be of about 5 K for the YBCO film. Such notable temperature change should be easily detected by the PPMS thermometer, while it was not the case. Thus, we can conclude that the critical current density drop is not governed by temperature

effects. Hence, we shell focus on magnetic nature of the fluctuations.

There are at least three sources of small magnetic field perturbations, which can arise during MPMS and PPMS measurements: (i) inhomogeneities of the magnetic field along the axis of the magnet (hereafter, assigned as z-axis), thus any movement of the superconductor along the z-axis (MPMS scan, VSM oscillations) would expose the superconductor to the field inhomogeneities; (ii) inhomogeneities of the magnetic field in the plane perpendicular to the z-axis, hence any displacement from the perfect z-axis movement would be felt by the superconductor; (iii) tilting of the superconductor relative to external magnetic field. The first two reasons are the consequences of the geometry of the MPMS/PPMS superconducting magnets, whereas the third reason might arise due to various mechanical imperfections of vibration mechanism. The first reason is more relevant to the MPMS measurements with its relatively long scan length (typically, 4 cm).[15] The superconductor oscillations along the z-axis upon PPMS VSM measurements are more than order of magnitude smaller, thus all three sources of field perturbations are likely to be equally important. Whereas the reasons leading to perturbations (i) are obvious, the displacements from the z-axis (ii) and the tilt of the superconductor (iii) can be expected due to in-plane swings of the sample rod upon sample oscillations in PPMS.[67] Both processes (ii) and (iii) may happen if the sample in the holder tilts slightly away from the z-axis. First, the sample can shift relatively its central position by up to 2 mm, being limited by the size of the pick-up coil (note, the sample lateral size is 5 mm). Second, the sample would tilt with respect to the direction of the magnetic field up to $\sim 0.5^\circ$ (as the result of the maximal shift).

In general, periodic movements of a superconductor in an inhomogeneous magnetic field cause redistribution of vortices and corresponding supercurrents. Redistribution of vortices and supercurrents is the subject to FLL dynamics and pinning properties. The supercurrents generated by these oscillations depend on the level of field inhomogeneities and the amplitude of the oscillations. In the case of the tilting of the superconductor relative to the z-axis, this process reminds the so-called flux-line walking described in Ref. 68 and observed in Refs. 17, 18, and 69. The small in-plane periodic field is considered to "shake" vortices out of pinning centres and force their relaxation.[65,68,70] A small ac current is induced by in-plane magnetic field oscillations (resulting from magnetic field direction deviation from sample's z-axis) tends to tilt vortices at each cycle of the oscillations, so that FLL is forced into more equilibrium position decreasing $\vec{\nabla} \times \vec{\mathbf{B}}$. If the frequency of oscillations would increase, it leads to more periods of relaxation happening over the same period of time and hence to a stronger decrease in magnetization (J_c) and B_{irr}. Qualitatively, it agrees with the reduction of the irreversible magnetization and the drop of the critical current density observed in Ref. 62. To an extent, this shaking process may also remind our experiments in PPMS. However, in our case the frequency range is more than order of magnitude lower, as well as the frequency increase reduces the irreversibility field to a certain constant value B_{irr}^{T} (Eq. (7)).

The oscillations along z-axis in a slightly inhomogeneous field, as well as tilting of the superconductor relative to the z-axis are somewhat similar to effects which may be expected for Vibrating Reed (VR) experiments in perpendicular fields.[71,72] The field inhomogeneity (generating ac field) would develop small perturbation of FLL which would travel through the superconductor depending on the sample geometry and ac field orientation according to the diffusivity of the magnetic flux.[73] The damping peak obtained upon Vibrating Reed measurements at a certain constant diffusivity $D = \rho/\mu_0$, being equivalent to the peak obtained in the imaginary part of the ac susceptibility measurements, determines the irreversibility (or depinning) line of FLL ($\mu_0 = 4\pi \times 10^{-7}$ Henry/m is the permeability of free space). The depinning peak corresponds to the onset of the resistivity (ρ) during transport current measurements,[26] arising due to vortex movements. However, we show that the effect caused by the sample vibration in PPMS VSM is different from the expected from the VR technique. Magnetic flux diffuses through the sample with certain diffusion times, which can be estimated according to Refs. 73–75: $\tau \simeq \mu_0 l_{3i}^2/\pi^2\rho$, where l_{3i} is an effective diffusion mode and $\rho \sim 10^{-14}$ to 10^{-12} Ω m according to the current densities and electric field criteria in our film. For ac susceptibility measurements,[2,76] the transverse ac mode for the flux movement (diffusion) is $l_{3i}^2 \simeq w_p d_p$, where w_p—width of the sample (5 mm) and d_p—thickness of the sample (450 nm), so $\tau \sim 10^{-4}$ to 10^{-2} s. This diffusion time can indeed be comparable to the period of the sample oscillation $1/f \sim 10^{-2}$ to 1 s. However, in this case the irreversibility field should increase in increasing frequency as shown in Refs. 76 and 77, which contradicts to our PPMS measurements. This contradiction and some similarity to magnetization relaxation observed upon "shaking" of flux-lines indicate that the key-factor affecting the J_c behaviour as a function of PPMS frequency is the ac component parallel to the film surface. This means that the inhomogeneity perpendicular to the z-axis of the magnet or tilt of the sample are of importance. However, the out-of--plane inhomogeneity can also introduce the in-plane ac-field component during sample vibration.

Thus, no existing explanations are applicable to treat the effects arising due to the low frequency vibrations in PPMS VSM. The highest degree of similarity to our case seems to be resembled by the walking flux lines in small perpendicular ac fields.[18,68] It leads to periodic pinning potential reduction due to additional ac currents, which in our case have much lower frequencies and effectively reduce B_{irr} only up to around 50 Hz. It is however possible to empirically describe the observed relaxation induced by the vibrations with the corresponding "instrumentally" induced decrease of $E_{\mathrm{cr,}}$ which can be derived from our model (Eq. (6)). Note, E_{cr} would conventionally be determined by sample size and the field sweep rate ($\sim s \times dB_a/dt$),[57] which is apparently achieved at $f \to 0$ with $E_{\mathrm{cr}} \simeq 10^{-5}$ V/m for $dB_a/dt = 5$ mT/s (Fig. 4). It is possible to directly fit the model to the obtained results at any frequency to acquire the corresponding E_{cr}. However, it is easier to use Fig. 2, which can provide E_{cr} according to the measured B_{irr}. Within the frequency range from 60 Hz to 40 Hz (the lower limit being the VSM default

frequency), the $E_{cr} \sim 10^{-10}$ V/m. This behaviour depends on the field sweep rate as well, which requires corresponding recalculation of the $B_{irr}(E_{cr})$ curve in Fig. 2. Importantly, this sweep rate dependence suggests that we should consider dynamic processes associated with a driven FLL, which could be the key to understanding the observed effects. It is also notable that in the case of work in Ref. 18, the FLL shaking was applied *after* sweeping the field to a constant field set point and then measured, while our case is truly dynamic with continuous field sweeping and simultaneous measurements of the vibrating superconductor.

VIII. CONCLUSION

In conclusion, a model for critical current density in YBCO thin films based on the pinning of flux line lattice on out-of-plane edge dislocations and Kim-Anderson vortex creep has been outlined. The advantage of the model is that it involves the electric field criterion of the corresponding measurement technique. This criterion enables the qualitative and quantitative comparison of experimental data obtained by different techniques. In this work, we have analysed the transport current technique, as well as magnetization measurements in quasi-equilibrium regime (MPMS) dynamic regime (PPMS VSM). The model has successfully been verified in the case of the transport and MPMS magnetization measurements. For these techniques, the values of the electric field criteria obtained within the model are well consistent with the experimental ones. On the other hand, the large difference between the model and experimental $J_c(B_a)$ curves observed for PPMS VSM magnetization measurements could not be explained by the model, unless the frequency of the superconducting sample vibrations is considered. These vibrations have exhibited significant influence on J_c behaviour, which could not be described by any existing model or theory. An empirical adjustment of the frequency dependent measurements has been proposed on the basis of the $B_{irr}(E_{cr})$ diagram derived from the model. The nature of the J_c drop with increasing vibration frequency is discussed in terms of (i) magnetic field inhomogeneities and (ii) the sample displacement and/or tilt with respect to the magnet axis. Movements of the samples in the inhomogeneous magnet fields will lead to additional driving forces inserted on the (driven) vortex lattice in the superconductors, which results in the J_c and B_{irr} degradation. A further analysis is required to understand and quantitatively explain the behaviour observed.

ACKNOWLEDGMENTS

This work is supported by the Australian Research Council via A. V. Pan's Discovery Projects (DP0879933 and DP110100398).

[1]E. M. Gyorgy *et al.*, Appl. Phys. Lett. **55**, 283 (1989).
[2]F. Gomory, Supercond. Sci. Technol. **10**, 523 (1997).
[3]Ch. Jooss *et al.*, Rep. Prog. Phys. **65**, 651 (2002).
[4]T. H. Johansen *et al.*, Phys. Rev. B **54**, 16264 (1996).
[5]G. Blatter *et al.*, Rev. Mod. Phys. **66**, 1125 (1994).
[6]P. Anderson and Y. Kim, Rev. Mod. Phys. **36**, 39–43 (1964).
[7]D. Dew-Hughes, Cryogenics **28**, 674 (1988).
[8]V. Calzona *et al.*, Supercond. Sci. Technol. **6**, 46 (1993).
[9]N. Savvides, Physica C **165**, 371 (1990).
[10]Y. Yeshurun and A. P. Malozemoff, Phys. Rev. Lett. **60**, 2202 (1988).
[11]I. A. Golovchanskiy *et al.*, Supercond. Sci. Technol. **24**, 105020 (2011).
[12]V. M. Pan *et al.*, Phys. Rev. B **73**, 054508 (2006).
[13]V. M. Pan *et al.*, Cryogenics **33**, 21 (1993).
[14]A. V. Pan, S. V. Pysarenko, D. Wexler, S. Rubanov, and S. X. Dou, IEEE Trans. Appl. Supercond. **17**, 3585 (2007).
[15]D. A. Luzhbin *et al.*, Phys. Rev. B **69**, 024506 (2004).
[16]R. G. Mints, Phys. Rev. B **53**, 12311 (1996).
[17]N. Avraham *et al.*, Nature **411**, 451 (2001).
[18]M. Willemin *et al.*, Phys. Rev. B **58**, R5940 (1998).
[19]M. Willemin *et al.*, Phys. Rev. Lett. **81**, 4236 (1998).
[20]K. A. Muller, M. Takashige, and J. G. Bednorz, Phys. Rev. Lett. **58**, 1143 (1987).
[21]D. S. Fisher, M. P. A. Fisher, and D. A. Huse, Phys. Rev. B **43**, 130 (1991).
[22]A. Houghton, R. A. Pelcovits, and A. Sudbo, Phys. Rev. B **40**, 6763 (1989).
[23]L. Krusin-Elbaum *et al.*, Phys. Rev. Lett. **72**, 1914 (1994).
[24]M. Tinkham, Phys. Rev. Lett. **61**, 1658 (1988).
[25]G. T. Seidler *et al.*, Physica C **183**, 333 (1991).
[26]A. V. Pan, F. Ciovacco, P. Esquinazi, and M. Lorenz, Phys. Rev. B **60**, 4293 (1999).
[27]T. Aytug *et al.*, Phys. Rev. B **74**, 184505 (2006).
[28]O. Polat *et al.*, Phys. Rev. B **84**, 024519 (2011).
[29]C. V. Varanasi, P. N. Barnes, and J. Burke, Supercond. Sci. Technol. **20**, 1071 (2007).
[30]S. Oh *et al.*, J. Appl. Phys. **102**, 043904 (2007).
[31]F. Lu, F. Kametani, and E. E. Hellstrom, Supercond. Sci. Technol. **25**, 015011 (2012).
[32]D. C. Larbalestier *et al.*, Nature **410**, 186 (2001).
[33]L. Cooley, Xu. Song, and D. C. Larbalestier, IEEE Trans. Appl. Supercond. **13**, 3280 (2003).
[34]A. V. Pan *et al.*, Appl. Phys. Lett. **88**, 232506 (2006).
[35]D.-X. Chen and R. B. Goldfarb, J. Appl. Phys. **66**, 2489 (1989) (Taylor and Francis, London, 1972).
[36]O. V. Shcherbakova, A. V. Pan, D. Wexler, and S. X. Dou, IEEE Trans. Appl. Supercond. **17**, 2790 (2007).
[37]O. V. Shcherbakova *et al.*, Supercond. Sci. Technol. **21**, 015005 (2008).
[38]S. Zhou, A. V. Pan, J. Horvat, M. J. Qin, and H. K. Liu, Supercond. Sci. Technol. **17**, S528 (2004).
[39]F. M. Sauerzopf, H. P. Wiesinger, and H. W. Weber, Cryogenics **30**, 650 (1990).
[40]S. R. Foltyn *et al.*, Nature Mater. **6**, 631 (2007).
[41]S. J. Pennycook *et al.*, Physica C **202**, 1 (1992).
[42]R. Wordenweber, Supercond. Sci. Technol. **12**, R86–R102 (1999).
[43]X.-Y. Zheng *et al.*, Phys. Rev. B **45**, 7584 (1992).
[44]H. Hilgenkamp and J. Mannhart, Rev. Mod. Phys. **74**, 485 (2002).
[45]B. Dam, J. M. Huijbregtse, and J. H. Rector, Phys. Rev. B **65**, 064528 (2002).
[46]F. C. Klaassen *et al.*, Phys. Rev. B **64**, 184523, (2001).
[47]V. M. Pan and A. V. Pan, "Vortex matter in superconductors," Fiz. Niz. Temp. **27** (Russian), 991 (2001) [Low Temp. Phys. **27**, 732 (2001)].
[48]B. Dam *et al.*, Nature **399**, 439 (1999).
[49]S. V. Pysarenko *et al.*, J. Appl. Phys. **107**, 09E118 (2010).
[50]V. V. Schmidt, *The Physics of Superconductors* (Springer-Verlag Berlin, Heidelberg, 1997).
[51]A. V. Pan and S. X. Dou, Phys. Rev. B **73**, 052506 (2006).
[52]A. V. Pan, *et al.*, Physica C **407**, 10 (2004).
[53]A. V. Pan, S. V. Pysarenko, and S. X. Dou, IEEE Trans. Appl. Supercond. **19**, 3391 (2009).
[54]P. Paturi *et al.*, J. Appl. Phys. **105**, 023904 (2009).
[55]Y. Yeshurun, A. P. Malozemoff, and A. Shaulov, Rev. Mod. Phys. **68**, 911 (1996).
[56]A. Gurevich and E. H. Brandt, Phys. Rev. Lett. **73**, 178 (1994).
[57]E. H. Brandt, Phys. Rev. B **52**, 15442 (1995).
[58]A. A. Zhukov *et al.*, Cryogenics **33**, 142 (1993).
[59]A. O. Caplin *et al.*, Supercond. Sci. Technol. **7**, 412 (1994).
[60]I. A. Golovchanskiy *et al.*, Physica C **479**, 151 (2012).
[61]J. Horvat *et al.*, J. Appl. Phys. **96**, 4342 (2004).

[62]A. Schilling, H. R. Ott, and Th. Wolf, Phys. Rev. B **46**, 14253 (1992).
[63]F. J. Blunt *et al*., Phys. C **175**, 539 (1991).
[64]A. E. Koshelev and A. I. Larkin, Phys. Rev. B **52**, 13559 (1995).
[65]G. P. Mikitik and E. H. Brandt, Phys. Rev. B **69**, 134521 (2004).
[66]J. Bardeen and M. J. Stephen, Phys. Rev. **140**, A1197 (1965).
[67]Quantum Design, private communications.
[68]E. H. Brandt and G. P. Mikitik, Phys. Rev. Lett. **89**, 027002 (2002).
[69]M. A. R. LeBlanc, S. Celebi, and M. Rezeq, Physica C **361**, 251 (2001).
[70]E. H. Brandt, Phys. Rev. B **48**, 6699 (1993).
[71]P. Esquinazi, J. Low Temp. Phys. **85**, 139 (1991).
[72]J. Kober, A. Gupta, P. Esquinazi, H. F. Braun, and E. H. Brandt, Phys. Rev. Lett. **66**, 2507 (1991).
[73]E. H. Brandt, Z. Phys. B **80**, 167 (1990).
[74]M. Ziese, P. Equinazi, and H. F. Braun, Supercond. Sci. Technol. **7**, 869 (1994).
[75]E. H. Brandt, Phys. Rev. Lett. **68**, 3769 (1992).
[76]H. Salamati and K. Kameli, J. Magn. Magn. Mater. **278**, 237 (2004).
[77]K. H. Muller, Physica C **168**, 585 (1990).